Journal of Computational and Applied Mechanics, Vol. 8., No. 2., (2007), pp. 135–148

INFLUENCE OF A CRUCIFORM ARRANGEMENT DOWNSTREAM STRIP-PLATE ON CROSSFLOW VIBRATION OF A SQUARE CYLINDER

Mizuyasu Koide, Naoto Kato, Shuichi Yamada, Yusuke Kawabata,
Tsutomu Takahashi, Masataka Shirakashi
Live Engineering Research Center, Niigata Sangyo University
4730 Karuigawa, Kashiwazaki, 945-1393, Japan
mkoide@ind.nsu.ac.jp

[Received: January 15, 2007]

Abstract. In earlier works, the present authors found that the Kármán vortex excitation of a circular cylinder is effectively suppressed by setting another cylinder in cruciform arrangement downstream with a gap-to-diameter ratio s/d less than 0.5, and that new vortex excitations are induced by two types of longitudinal vortices shedding periodically near the cross in higher velocity ranges. In this work, influence of a strip-plate set downstream in cruciform arrangement on the vibration of a square cylinder is investigated by wind tunnel experiments. The Kármán vortex excitation is well suppressed by the strip-plate with a width w equal to the side of square d when $s/d < 2$. Galloping is also completely suppressed by the plate when $s/d < 4$, except the range of $1 < s/d < 2$. In the latter range of s/d, a new vibration occurs and its maximum amplitude at s/d around 1.3 is double the original galloping. Flow visualization by tuft grid and velocity measurement show that this vibration is caused by longitudinal vortex shedding periodically near the cross which synchronizes with the cylinder motion, similar to the case of a two-circular-cylinder system.

Keywords: flow induced vibration, galloping, longitudinal vortex, vibration control, vortex excitation

Nomenclature

d	side-length of square cylinder = 26 mm
f_n	system natural frequency
f_v	vortex shedding frequency
f_{v0}	vortex shedding frequency for fixed systems
f_z	vibration frequency
Re	Reynolds number ($= Ud/\nu$)
s	gap between bodies
St	Strouhal number ($= f_v d/U$)
St_0	Strouhal number for fixed systems ($= f_{v0} d/U$)
S_u	spectrum of velocity u
U	free stream velocity

u	velocity component in the x-direction
w	width of downstream strip-plate
Z	z-displacement of upstream cylinder
Z_{rms}	root-mean-square value of Z
${Z_{rms}}^*$	Z_{rms} normalized by Z_{rms} of single cylinder
δ	logarithmic damping factor
ν	kinematic viscosity of fluid

1. **Introduction**

Since vibrations of cylindrical bodies in fluid flow have caused many serious accidents in mechanical and structure engineering, various methods for controlling flow-induced vibration of a cylindrical body have been proposed so far, such as suction holes on the surface of the body, tripping wires near separation points, a splitter plate in the wake, and so on [1]. The innumerable number of such techniques shows the practical importance of the phenomenon.

Tomita et al. [2] reported that the acoustic noise from a circular cylinder can be suppressed by setting another cylinder downstream in cruciform arrangement with a certain gap between them as shown in Figure 1. Inspired by Tomita's work, the present authors investigated the effect of the downstream cylinder on the Kármán vortex excitation of the upstream cylinder, and found that the vibration is effectively suppressed when the gap-to-diameter ratio s/d is less than around 0.5. However, it was also found that two types of longitudinal vortices, i.e. trailing vortex (Figure 1(a)) or necklace vortex (Figure 1(b)), shed periodically depending on the gap-to-diameter ratio and that these longitudinal vortices induce resonant excitation similar to the Kármán vortex excitation over respective velocity regions, several times higher than that of the latter [3, 4].

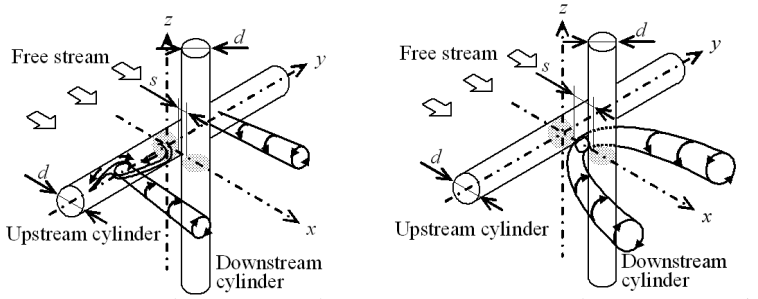

(a) Trailing vortex ($0 \leq s/d \leq 0.25$) (b) Necklace vortex ($0.25 \leq s/d \leq 0.5$)

Figure 1. Longitudinal vortices from a cruciform two circular cylinder system

In the case of a square cylinder, it is well known that another crossflow vibration called 'galloping' occurs at velocities higher than the Kármán vortex excitation caused by flow-elastic instability [1].

Recently, the present authors found that a cruciform arrangement downstream strip-plate with a width w equal to the side of the square d can suppress both the Kármán vortex excitation and the galloping, and induce a longitudinal vortex excitation [5]. The specific aim of this work is to investigate the effects of a cruciform downstream strip-plate on the crossflow vibration behaviour of a square cylinder in detail by using strip-plates with variable width in wind tunnel experiments.

2. **Experimental apparatus and measurement**

Arrangement of the experimental apparatus and the coordinate system used in this paper are shown in Figure 2. A blow down type wind tunnel with a test section of 0.32 m square cross-section (the upper and lower walls of the test section are not drawn in Figure 2 and a 1 m length is used. The turbulence level at the center of the test section is less than 0.6 % at $U = 2\ m/s$.

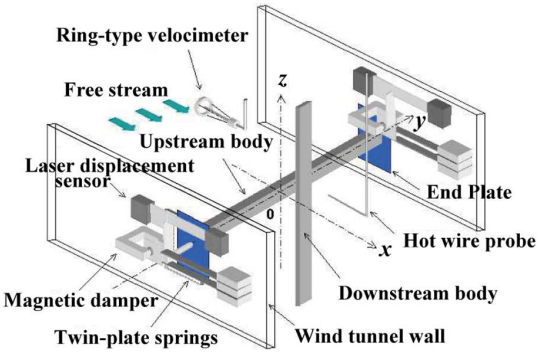

Figure 2. Arrangement of the experimental apparatus and the coordinate system

A rigid rod passes through slots on the side walls of the measuring section and is fixed rigidly or supported elastically at both ends outside the measuring section. In the latter setup, two twin-plate-springs are used as shown in Figure 2 so as to make its motion pure crossflow mode [6]. A square cross-section cylinder with a side-length $d = 26\ mm$ and a spanwise length $l_e = 318\ mm$ is fixed to the rod. End plates are attached to the cylinder to remove influence of flow through the slots [7].

A strip-plate is mounted rigidly on a traversing table set beneath the measuring section, which allows adjusting the gap s within an accuracy of 0.05 mm. The downstream strip-plate is spanned over the whole height of the measuring section. The width of the downstream strip-plate w is varied from 10 mm to 26 mm, while its thickness is fixed at 5 mm. Preliminary experiments have shown that the influence of the plate thickness is insignificant.

The natural frequency f_n and logarithmic damping factor δ are obtained by free damping oscillation in air otherwise at rest. The effective mass m_e is calculated from

f_n thus determined and the spring constant k measured separately. The free flow velocity U is measured by a ring-type velocimeter [8]. The vortex shedding frequency f_v is determined from a spectrum S_u of x-component velocity u, measured by using a hot-wire probe placed at an appropriate location to detect the periodic shedding of vortices.

The vertical displacement of the square cylinder, Z, is defined as the average of values measured by laser displacement sensors at the two ends of the supporting rod outside the measuring section (Figure 2). The tuft grid method is applied to observe the cross section of the longitudinal vortex in the wind tunnel.

3. **Kármán vortex excitation and galloping of an isolated square cylinder**

Vibration of the isolated square cylinder (i.e. without downstream strip-plate) and the vortex shedding frequency were measured at an increasing and then decreasing flow velocity.

Variation of spectra of velocity and displacement for the former case is shown in Figure 3.

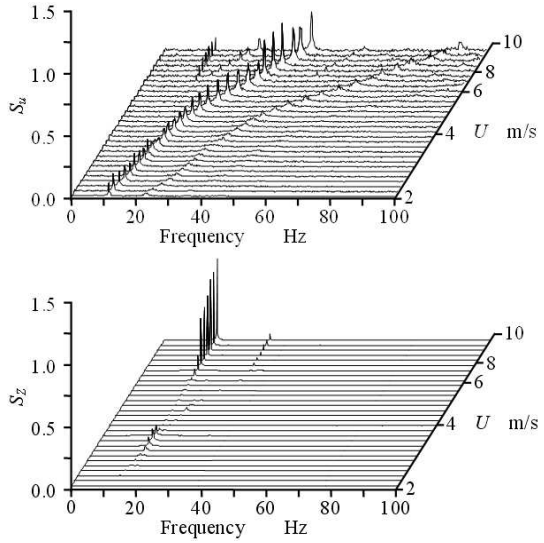

Figure 3. Variation of spectra of velocity and displacement with increasing U for isolated square cylinder ($f_n = 16.41\ Hz$, $\delta = 0.038$. Hot-wire probe position: $x/d = 1.5$, $y/d = 0$, $z/d = 0.4$)

As seen in this Figure, the cylinder oscillates essentially at its natural frequency irrespective of flow velocity U over the complete range of measurement. Meanwhile, the velocity spectra have a sharp peak at a frequency almost proportional with U, showing periodic Kármán vortex shedding.

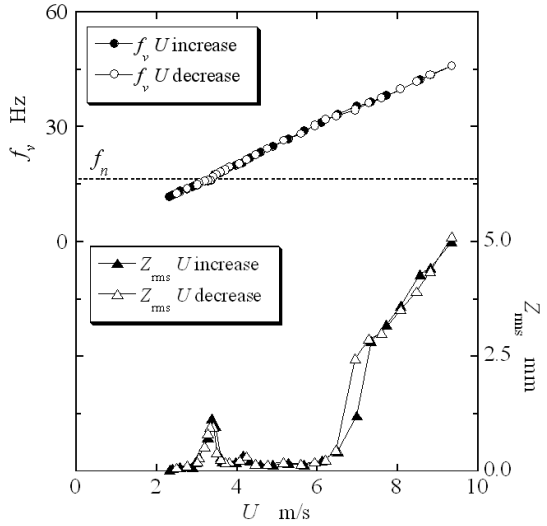

Figure 4. Vibration behaviour of an isolated square cylinder (f_n = 16.41 Hz, $\delta = 0.038$. Hot-wire probe position: $x/d = 1.5$, $y/d = 0$, $z/d = 0.4$)

In Figure 4, the oscillation amplitude expressed by the RMS value of z-displacement, Z_{rms}, and the vortex shedding frequency f_v, which is the dominant frequency of the spectrum in Figure 3, are plotted against the flow velocity U. As well known for the case of a single square cylinder, the Kármán vortex excitation and galloping are clearly observed in separated velocity regions in the Figure. The former is observed over a certain range of U around 3.4 m/s as seen in Figure 3, where the spectra of displacement Z and velocity u have a sharp peak at the frequency f_n, showing occurrence of the lock-in phenomenon. Meanwhile, the latter vibration increases with velocity and f_v is much higher than f_n. It should be noted here that the vibration frequency f_z is fixed at f_n over the complete velocity range of galloping, being much lower than the Kármán vortex shedding frequency f_v (see Figure 3). This fact, together with the fact that the frequency f_z of the Karman vortex excitation coincides with the structure frequency obtained in fluid otherwise at rest, is the common nature of flow induced vibration of a system with a low damping factor in a low density fluid such as in air flow [1, 9].

4. **Suppression of Kármán vortex excitation**

Vibration of the isolated square cylinder (i.e. without downstream strip-plate) and the vortex shedding frequency were measured at an increasing and then decreasing flow velocity.

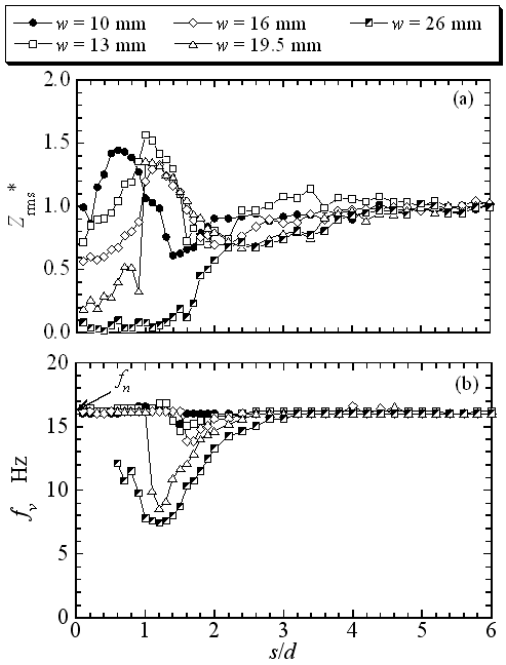

Figure 5. Effect of downstream strip-plate on the Kármán vortex excitation ($U = 3.4\ m/s$). (a) Vibration amplitude normalized by its value of isolated cylinder, (b) Vortex shedding frequency (Hot-wire probe position: $x/d = 1.5$, $y/d = 1.25$, $z/d = 0.4$)

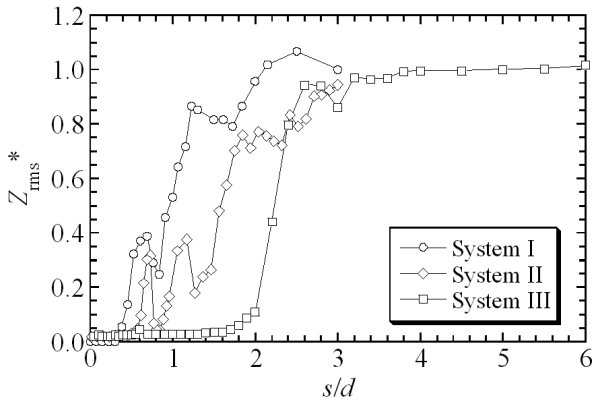

Figure 6. Suppression of Kármán vortex excitation for three systems. System I: Two circular cylinders ($U = 3.0\ m/s$, $f_n = 24.0\ Hz$, $\delta = 0.0166$), System II: Circular cylinder and strip-plate ($U = 2.6 m/s$, $f_n = 16.7 Hz$, $\delta = 0.0078$, $w/d = 1$), System III: Square cylinder and strip-plate ($U = 3.8\ m/s$, $f_n = 17.0\ Hz$, $\delta = 0.0690$, $w/d = 1$)

The results thus obtained are plotted against s/d in Figure 5 for five strip-plates with different widths, together with the vortex shedding frequency. Approaching the $w = 26\ mm$ plate ($w/d = 1$), the vibration begins to decrease when $s/d = 4$ and is almost completely suppressed when $s/d < 1.5$. However, this effect becomes weaker for narrower plates and it is paradoxical that the vibration amplitude becomes considerably larger than the original Kármán vortex excitation for plates with $w \leq 19.5\ mm$ over a certain region of $s/d < 1.5$. The vortex shedding frequency f_v in Figure 5(b) is seen to be considerably lower than f_n or to vanish when the vibration is small.

In Figure 6, the suppression of Kármán vortex excitation is compared for the cases of three different configuration cruciform systems with $w/d = 1$, i.e. System I: two circular cylinders, System II: circular cylinder and strip-plate, and System III: square cylinder and strip-plate (the present setting but supported by single plate springs) [10]. In this figure, ${Z_{rms}}^*$ begins to decrease around $s/d = 2 - 3$ for all the systems. Compared with the other two systems, i.e. System I and System II, the effect is strongest for System III in the sense that the maximum value of s/d to suppress the vibration is largest among the three.

5. **Suppression of galloping**

The suppression effect of the strip-plate on galloping was observed in the same way as for the Kármán vortex excitation described above. The velocity was set constant at 7.6 m/s selected as the representative value (see Figure 4) and the results are presented in Figure 7. Compared with the case of Kármán vortex excitation in Figure 5, the effect is more remarkable in that the vibration is completely suppressed with s/d as large as around four when $w/d = 1$. The maximum value of s/d where the vibration begins to become lower is smaller with the smaller width strip-plates. However, there appears again a large vibration when s/d is made still smaller, in the cases of $w = 10\ mm$, $13\ mm$ and $26\ mm$. This second vibration peak is indefinite for the plates with intermediate width plates ($w = 16\ mm$ and $19.5\ mm$). In the case of the $w = 26\ mm$ plate, the peak value of the second vibration in the range of $s/d = 1.2 - 1.5$ is larger than double the original galloping. The vortex shedding frequency f_v in this range of s/d is equal to f_n for the $w = 26\ mm$ plate, while f_v for the second vibration peak it is slightly higher than the value of single cylinder for the $w = 10\ mm$ and $13\ mm$ plates. Note that the vibration frequency f_z is fixed at f_n for all the measurements shown in Figure 7.

The results shown in Figure 7 imply that the origin of the second vibration peak for the $w = 26\ mm$ plate is the longitudinal vortex similar to those observed in the two circular cylinder system as shown in Figure 1. In contrast, the second vibration of the $w = 10\ mm$ and $13\ mm$ plates are not attributed to the longitudinal vortex but may be attributed to galloping.

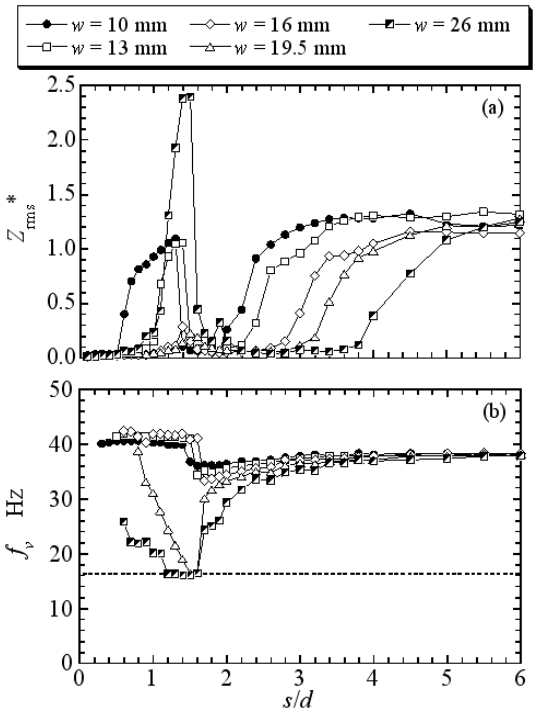

Figure 7. Effect of downstream strip-plate on galloping ($U = 7.6\ m/s$). (a) Vibration amplitude normalized by its value of isolated cylinder, (b) Vortex shedding frequency (Hot-wire probe position: $x/d = 1.5$, $y/d = 1.25$, $z/d = 0.4$)

6. **Longitudinal vortex excitation**

The vibration and the vortex shedding frequency of the square cylinder with the $w = 26\ mm$ plate set at $s/d = 1.2$, the gap at which the second vibration is clearly observed in Figure 7, were measured at an increasing and then decreasing flow velocity U.

Variation of spectra of velocity and displacement for the increasing U is shown in Figure 8. Compared with the isolated square cylinder (Figure 3), spectrum peaks in S_Z around $U = 3.5\ m/s$ which correspond to Kármán vortex excitation disappear. Instead, sharp spectrum peaks appear in S_Z when $6.5\ m/s < U < 8\ m/s$.

Dominant frequencies of the spectra S_u in Figure 8 are plotted against the flow velocity U as a vortex shedding frequency f_v in Figure 9, together with the oscillation amplitude expressed by the RMS value of z-displacement, Z_{rms}. As seen in Figure 9, both the Kármán vortex excitation and the galloping in Figure 4 disappear and a

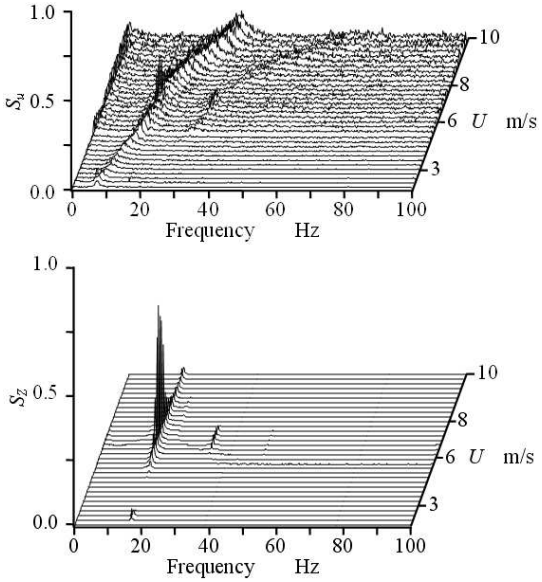

Figure 8. Variation of spectra of velocity and displacement with increasing U for the square cylinder with a strip-plate ($f_n = 16.41\ Hz$, $\delta = 0.038$, $w/d = 1$, $s/d = 1.2$, Hot-wire probe position: $x/d = 1.5$, $y/d = 1.25$, $z/d = 0.4$)

new vibration is induced instead over a velocity range of $U = 6.5 - 8\ m/s$, where the peak frequency f_v in the velocity spectrum remains fixed on $f_z = f_n$.

Except for this range of U, f_v increases proportionally with U and is much lower than that of the isolated cylinder. Therefore, the new vibration is inferred to be caused by the longitudinal vortices.

To confirm this, the flow downstream the cross of the vibrating square cylinder was visualized by the tuft-grid method as shown in Figure 10. There, the cross-section of longitudinal vortex is clearly observed at the two anti-phase instants, (a) and (b), in a period of cylinder displacement Z. It is clearly seen that the pattern is symmetric about the $x - z$ plane in photos (a) and (b), and that the vortex pattern is observed only one side of positive or negative z region. However, it cannot be discerned whether the longitudinal vortex in Figure 10 is the necklace or the trailing vortex shown in Figure 1.

7. **Characteristics of longitudinal vortex from fixed system**

The square cylinder in the same setting as in Figure 10 was fixed rigidly and the hot-wire probe was traversed towards the side wall parallel to the y-axis. Figure 11 shows velocity spectra for various spanwise positions thus obtained. A sharp peak

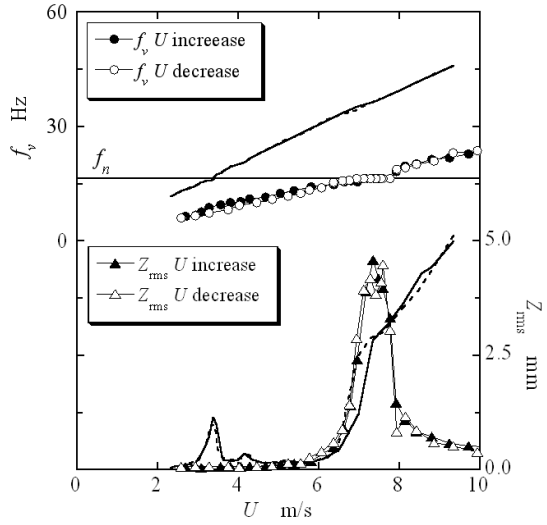

Figure 9. f_v and Z_{rms} versus U for the square cylinder with a strip-plate. $fn = 16.41\ Hz$, $\delta = 0.038$, $w/d = 1$, $s/d = 1.2$, Hot-wire probe position: $x/d = 1.5$, $y/d = 1.25$, $z/d = 0.4$, solid line: isolated square cylinder (U increase), broken line: isolated square cylinder (U decrease)

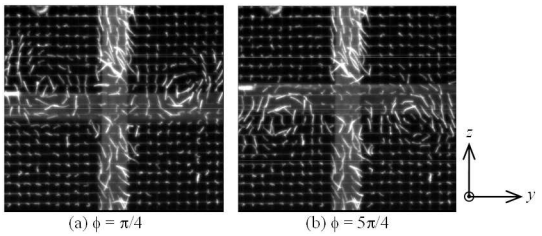

Figure 10. Longitudinal vortices synchronizing with square cylinder oscillation in wind tunnel, viewed from downstream ($w/d = 1$, $s/d = 1.2$, $\delta = 0.069$, single-plate-springs, Re = 13200, Grid position: $x/d = 2.7$)

appears in S_u when $y/d < 3$ and no peak is observed beyond this position, showing that the Kármán vortex shedding is removed by the downstream plate.

The hot-wire probe was set at the position where the peak in spectrum S_u is most clearly observed in Figure 11, and the gap s was varied while the velocity U was set constant. The spectra and the peak frequency f_{v0} thus obtained are shown in Figure 12, the latter being normalized by its isolated cylinder value $f_{v0\infty}$ and compared with the results by Fox [11] on a two-square-cylinder system. The peak in S_u in the region

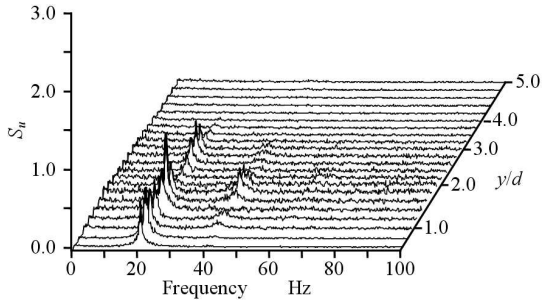

Figure 11. Velocity spectra for various spanwise position($w/d = 1$, $s/d = 1.2$, $U = 7.6\ m/s$, Probe position: $x/d = 1.5$, $y/d = 0.8$~5.0, $z/d = 0.4$)

$s/d > 5$ is caused by the Kármán vortex with a frequency essentially equal to that of the isolated cylinder. The continuous nature of the changes in the shape and peak frequency of S_u in the region $2 < s/d < 6$ implies that the Kármán vortex sheds there and that its frequency and regularity become lower by the interference of the downstream plate.

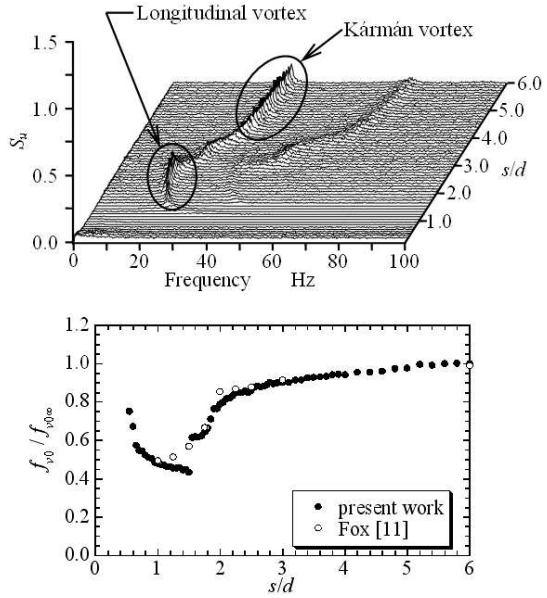

Figure 12. Variation of velocity spectrum and its peak frequency against gap for fixed system ($w = 26\ mm$, $U = 7.6\ m/s$, Probe position: $x/d = 1.5$, $y/d = 1.25$, $z/d = 0.4$)

The abrupt changes in S_u and f_{v0} at around $s/d = 1.7$ show that the vortex structure becomes different from that of Kármán vortex when s/d is smaller than this value. The observation of flow as seen in Figure 10, and also by Fox [11], may suggest that the low frequency vortex in the region $s/d < 1.7$ is the necklace vortex as shown in Figure 1 (b). The peak frequency f_{v0} in S_u near the cross of the fixed system is reduced to the Strouhal number S_{t0} and plotted against the Reynolds number Re as shown in Figure 13, together with results for the other two configuration systems. Figures 11 - 13 verify that the periodic shedding of the longitudinal vortex is inherent in this boundary condition but not induced by the cylinder vibration, and show that the Strouhal number of the longitudinal vortex is $0.05-0.06$, while that of the Kármán vortex is around 0.13.

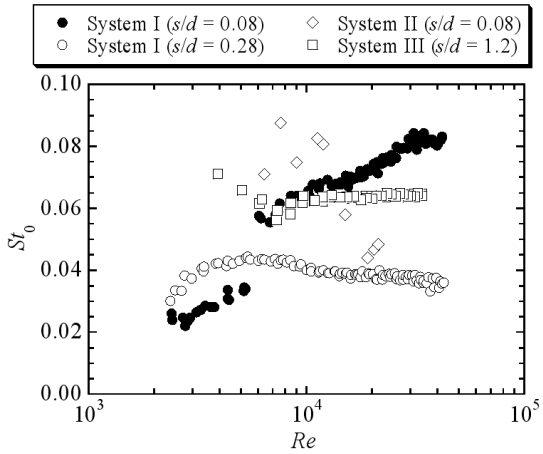

Figure 13. Strouhal number of longitudinal vortices versus Reynolds number for fixed system. System I: Two circular cylinders [5], System II: Circular cylinder and strip-plate [5], System III: Square cylinder and strip-plate (present system)

8. **Conclusions**

Wind tunnel experiments were carried out to investigate the interference effect of a strip-plate set downstream in cruciform arrangement on the crossflow vibration behavior of a square cylinder in uniform flow. The results are compared with different configuration systems, i.e. cruciform two-circular-cylinder and circular-cylinder/strip-plate systems. The conclusions are summarized as follows.

1. Both the Kármán vortex excitation and the galloping of the square cylinder are effectively suppressed by the downstream strip-plate in spite of the fact that the mechanisms of the two vibrations are totally different.

2. A longitudinal vortex excitation similar to that observed for the two-circular-cylinder system is induced by the downstream strip-plate over a range of non-dimensional gap s/d considerably larger compared with the latter.

Generally speaking, the effect of a cruciform downstream strip-plate is stronger in the square-cylinder/strip-plate configuration in the sense that the range of s/d to influence the vibration is much larger than in the other two cases. The most remarkable effect is that galloping is completely suppressed by the $w/d = 1$ strip-plate even when the gap is as large as four times the side length of the square.

However, the above effects of the downstream plate are largely different when the width of the plate is smaller. Since the flow around the cross is of highly three dimensional nature accompanied by periodic vortex shedding of longitudinal vortices superimposed by turbulence, mechanisms to cause the influences on vibration are left for further investigations.

Acknowledgement. The authors wish to thank Mr. Ohta, M. for his experimental supports.

REFERENCES

1. Blevins, R.D.: *Flow-Induced Vibration*. 2nd Ed., Van Nostrand, 1990.
2. Tomita, Y., Inagaki, S., Suzuki, S. and Muramatsu, H.: Acoustic characteristics of two circular cylinders forming a cross in uniform flow. *JSME International Journal*, **30**, (1987), 1069-1079.
3. Shirakashi, M., Bae, H.M., Sano, M., and Takahashi, T.: Characteristics of periodic vortex shedding from two cylinders in cruciform arrangement. *Journal of Fluids and Structures*, **8**, (1994), 239-256.
4. Takahashi, T., Baranyi, L., and Shirakashi, M.: Configuration and frequency of longitudinal vortices shedding from two cylinders in cruciform arrangement. *Journal of the Visualization Society of Japan*, **19**(75), (1999), 328-336.
5. Kato, N., Koide, M., Takahashi, T. and Shirakashi, M.: Influence of cross-sectional configuration on the longitudinal vortex excitation of the upstream cylinder in cruciform two-cylinder system. *Journal of Fluid Science and Technology*, **1**(2), (2006), 126-137.
6. Kamimura, Y., Koide, M., Takahashi, T. and Shirakashi, M.: Effect of slenderness on cross-flow oscillation of a rectangular cylinder supported by cantilever in uniform flow, Proceedings of CMFF'03, The 12th International Conference on Fluid Flow Technologies, (2001), pp. 399-406.
7. Shirakashi, M., Ishida, Y. and Wakiya, S.: Higher velocity resonance of circular cylinder in crossflow. *Journal of Fluids Engineering*, **108**, (1986), 392-396.
8. Koide, M., Takahashi, T. and Shirakashi, M.: Development of a Ring-Type Vortex Anemometer for Low-Velocity Wind Tunnel Experiments. *Bulletin of Japan Society of Mechanical Engineers*, (in Japanese), 67, 657, B, (2001), 1105-1111.
9. Sarpkaya, T.: A critical review of the intrinsic nature of vortex-induced vibrations. *Journal of Fluid and Structures*, **19**, (2004), 389-447.

10. Kato, N., Koide, M., Takahashi, T. and Shirakashi, M.: Interference of downstream body on the oscillation behavior of a circular and a square cylinder in uniform flow, Proceedings of PVP (2005), PVP2005-71517, July 17-21, Denver, Colorado USA.

11. Fox, T.A.: Interference in the wake of two square-section cylinders arranged perpendicular to each other. *Journal of Wind Engineering and Industrial Aerodynamics*, **40**(1), (1992), 75-92.